Spatial variations in sedimentary N-transformation rates in the North Sea (German Bight)

Alexander Bratek[1,2], Justus E.E. van Beusekom[1], Andreas Neumann[1], Tina Sanders[1], Jana Friedrich[1], Kay-Christian Emeis[1,2] and Kirstin Dähnke*[1]

[1] Helmholtz-Zentrum Geesthacht, Institute for Coastal Research, Geesthacht, Germany
[2] University of Hamburg, Center for Earth System Research and Sustainability, Institute for Geology, Hamburg, Germany

Correspondence to: kirstin.daehnke@hzg.de

Abstract

In this study, we investigate the role of sedimentary N cycling in the Southern North Sea. We present a budget of ammonification, nitrification and sedimentary NO_3^- consumption / denitrification in contrasting sediment types of the German Bight (Southern North Sea), including novel net ammonification rates. We incubated sediment cores from four representative locations in the German Bight (permeable, semi-permeable and impermeable sediments) with labeled nitrate and ammonium to calculate benthic fluxes of nitrate and ammonium and gross rates of ammonification and nitrification. Ammonium fluxes generally suggest oxic degradation of organic matter, but elevated fluxes at one sampling site point towards the importance of bio-irrigation or short-term accumulation of organic matter. Sedimentary fluxes of dissolved inorganic nitrogen are an important source for primary producers in the water column, supporting ~7 to 59 % of the average annual primary production, depending on water depth.

We find that ammonification and oxygen penetration depth are the main drivers of sedimentary nitrification, but this nitrification is closely linked to denitrification. One third of freshly produced nitrate in impermeable sediment and two-thirds in permeable sediment were reduced to N_2. The semi-permeable and permeable sediments are responsible for ~68 % of the total benthic N_2 production rates, which, based solely on our data, amounts to ~1030 t N d^{-1} in the southern North Sea. Thus, we conclude that semi-permeable and permeable sediments are the main sinks of reactive N, counteracting eutrophication in the southern North Sea (German Bight).

1 Introduction

The continental shelves and coastal margins make up for <9 % of the total area of ocean surface, but are responsible for vast majority of the biogeochemical cycling both in the water column and in the sediments (Jorgensen, 1983). For instance, 30 % of global marine primary production occurs in coastal, estuarine and shelf systems (LOICZ, 1995), and nutrient regulation in shelf sediments is a particularly valuable ecosystem service (Costanza et al., 1997).

The German Bight is part of the southern North Sea and is bordered by densely populated and industrialized countries, and receives large amounts of nutrients via river discharge (e.g., Rhine, Maas, Elbe, Weser, Ems) (Los et al., 2014). This caused clear eutrophication symptoms such as phytoplankton blooms, oxygen deficiencies and macrobenthos kills especially during the 1980s (Hickel et al., 1993; von Westernhagen et al., 1986) in the North Sea. In the adjacent Wadden Sea intense phytoplankton blooms, a possible decrease of seagrass and massive blooms of opportunistic macroalgae were attributed to eutrophication (e.g. Cadée and Hegemann, 2002). Since the mid 1980s, the nitrogen (N) loads into the German Bight have been decreasing, but the entire SE North Sea is still flagged as an eutrophication problem area (OSPAR, 2010).

Nitrogen availability increases primary production on a variety of spatial and temporal scales. At present, major nitrogen sources for the Southern North Sea are agricultural and urban waste water, and to a lesser extent, a variety of reactive N emission (e.g., nitrogen oxides from burning fossil) (Emeis et al., 2015).

Internal N cycling in sediments (e.g., assimilation, ammonification and nitrification) change the distribution and speciation of fixed N, but not the overall amount of N available for primary production (Casciotti, 2016). Reduction of reactive nitrogen through denitrification and anammox in anoxic conditions back to unreactive N_2, however, does remove N from the biogeochemical cycle (Neumann et al., 2017).

Because these eliminating processes are confined to suboxic and anoxic conditions, they only occur in sediments in the generally oxygenated North Sea. Due to its putative relevance as an ecosystem service, denitrification has been subject to many studies, but ammonification as a source of N to primary production so far received much less attention. This is in part due to the complexity created by coupled ammonification-nitrification in which different N processes, such as assimilation and denitrification, interact and affect the NH_4^+ and NO_3^- concentrations in pore waters. To our knowledge, no ammonification rates in the North Sea have been quantified, whereas nitrification rates in permeable sediments were found to be in the same order of magnitude as denitrification rates (<0.1 to ~3.0 mmol m^{-2} d^{-1}, Tab. 1) (Marchant et al., 2016). N loss in the German Bight has been studied by several authors (e.g. Deek et al., 2013) showing high spatial, temporal and seasonal variability.

The main N loss process in the North Sea is denitrification, whereas and anammox plays a minor role (Bale et al., 2014; Marchant et al., 2016). The main drivers of denitrification are organic matter content and permeability of the sediment (Neumann, 2012), and recent studies suggest that permeable sediments account for about 90 % of the total benthic NO_3^- consumption in the German Bight (Neumann et al., 2017).

Quantifying N dynamics based solely on changes in N concentrations provides limited insight into underlying reactions, as only net changes can be observed. Previous authors used different methods for determination of specific N rates. Lohse et al. (1993) used the acetylene block method, core flux incubations and isotope pairing in the early 1990s types to determine denitrification rates in a variety of sediment types (Tab. 1). Deek and co-authors (Deek et al., 2013; Deek et al., 2011) investigated N-turnover in the Wadden Sea and in the extended Elbe estuary using core flux incubations and isotope pairing. Marchant et al. (Marchant et al., 2016) measured denitrification rates in permeable sediments obtained from slurry incubations and percolated sediment cores. More recently, Neumann et al. (2017) used pore-water NO_3^- concentration gradient profiles to determine NO_3^- consumption rates in the German Bight.

Stable isotope techniques offer several approaches to quantify N turnover processes, and ^{15}N tracer studies have been widely used to determine N transformation rates (e.g. nitrification and denitrification) (Brase et al., 2018; Sanders et al., 2018). The isotope dilution method can be used to distinguish between net and gross rates and so help to unravel several N-processes such as ammonification and assimilation or nitrification and denitrification. ^{15}N dilution $^-$ (Koike and Hattori, 1978; Nishio et al., 2001) can be used to estimate gross N transformation rates by measuring the isotopic dilution of the substrate and product pools, respectively (e.g. Burger and Jackson, 2003). In this study, we used the isotope dilution method with labeled NH_4^+ and NO_3^- in separate sediment cores to measure gross ammonification and gross nitrification. The net rates are determined by the sediment nutrient fluxes. To measure denitrification we determined the produced N_2 independently of the labelling in the core. Sediment core incubation experiment setup can never reproduce the identical conditions related to the advective processes in permeable sediments. Nevertheless this method has advantages over just balancing sediment-water exchanges: (1) The appearance of ^{15}N in the NH_4^+ pool during the incubation allows an estimate of ammonification rates, (2) the isotopic dilution of NO_3^- tracks nitrification rates,

This study is conducted within the project "North Sea Observation and Assessment of Habitats" (NOAH). One important aspect of the project is to investigate the biogeochemical status and functions of the sea floor, especially nitrogen cycling, to gauge the eutrophication mitigation potential in light of continuing high human pressures (https://www.noah-project.de).

In this paper, we investigate internal N rates of ammonification, nitrification and denitrification at four stations across sediment types (clay/silt, fine sand, coarse sand) in the German Bight (North Sea) during late summer (August/September) 2016. To assess the internal sediment N processes and the rates of reactive N release to the water column, we incubated sediment cores amended with $^{15}NH_4^+$ and $^{15}NO_3^-$. We quantify the benthic gross and net nitrification and ammonification rates and evaluate the environmental controls underlying spatial variabilities. We further discuss the role of ammonification as a source of reactive nitrogen for primary producers, of nitrification and of denitrification in the Southern North Sea.

2 Material and Methods

2.1 Study site and sampling strategy

The study site is in the German Bight (Southern North Sea), an area that is strongly influenced by nutrient inputs from large continental rivers. The salinity in the coastal zone of the North Sea ranges between ~30 and 35, and the average flushing time is 33 days (Lenhart and Pohlmann, 1997). The sampling was performed in August and September 2016 during R/V *Heincke* cruise HE-471 in the German Bight (Fig. 1).

The sampling sites are part of the NOAH (North Sea Assessment of Habitats) assessment scheme (Fig. 1). Samples were taken from 4 site (NOAH A, C, D and E) with different water depth and sediment characteristics (Table 2). The sites represent typical sediment types based on statistics of granulometric properties, organic matter content, permeability, and water depth assessed during former cruises (https://doi.org/10.1594/PANGAEA.846041). Organic matter and CN ratio data from cruises HE 383 (06/07.2012) and HE 447 (06.2015) were used.

2.2 core sampling and incubation

At each station (NOAH A, C,D and E) both water samples and sediment samples were taken. Water samples were taken with Niskin bottles attached to a CTD with additional chlorophyll and O_2 sensors. Sediment multicores equipped with acrylic tubes (PMA) with an inner diameter of 10 cm and a length of 60 cm were used. Four intact sediment cores from each station (exception: Station NOAH-D, only 3 cores could successfully be retrieved) were incubated in a gas tight batch-incubation setup for 24 hours (Fig. 2) in the ship's laboratory at in-situ temperature.(~19°C) directly after sampling. Cores were handled carefully to avoid disturbance that could alter benthic fluxes. Cores were incubated in the dark and the overlying site water was gently stirred with a magnetic stirrer, avoiding sediment resuspension. The overlying water column was adjusted to a height of 20 cm. Water temperature and oxygen concentration of the overlying water of sediment cores were measured continuously with optodes (PyroScience, Germany).

To measure gross ammonification, two sediment cores (Station NOAH-D 1 core only) were enriched with $^{15}NH_4^+$ (50 at-%,), the other two cores were amended with $^{15}NO_3^-$ (50 at-%) for an assessment of gross nitrification (Fig.

119   2). NH_4^+ and NO_3^- concentrations of the added tracer solution were adjusted to bottom water concentrations based

120   on nutrient data of previous cruises of the same location and time (later confirmed by nutrient analyses of site

121   water). For label addition, site water was replaced with the respective label solution. Due to the careful adjustment

122   of concentrations, incubations were done at a tracer level, and benthic fluxes should not be altered. ==The label==

123   ==addition was calculated aiming for a maximum enrichment of 5,000 ‰ in substrates.==

124   Samples were taken every 6 hours. Upon sampling, incubation water was filtered with a syringe filter (cellulose

125   acetate, Sartorius, 0.45 µm pore size) and frozen in exetainers (11.8 ml, Labco, High Wycombe, UK) at -20 °C for

126   later analyses of nutrients and stable isotope signatures ($\delta^{15}NH_4^+$, $\delta^{15}NO_3^-$). Additional samples for the analyses of

127   dissolved nitrogen (N_2) were taken without filtration, and were preserved in exetainers (5.9 ml, Labco, High

128   Wycombe, UK) containing 2 % of a $ZnCl_2$ solution (1 M). Samples were stored at 4 °C under water until analysis.

129   **2.3 Analyses**

130   **N_2 measurements by MIMS**

131   N_2 production was measured by a membrane inlet mass spectrometer (MIMS, inProcess Instruments), which

132   quantifies changes in dissolved N_2:Ar ratios (Kana et al., 1994) from all four cores. During the measurements, the

133   water samples were maintained in a temperature-controlled water bath (16 °C). For calibration, we measured

134   equilibrated water samples at four salinities, from 0 to 35 after each 10th water sample. We measured the production

135   of ^{28}N. The internal precision of the samples was <0.05 % for N_2/A_r analyses.

136   **Oxygen penetration depth**

137   The oxygen penetration depth in the sediment of each station was measured using microoptodes (50 µm tip size;

138   Presens, Germany). The optodes were moved vertically into the sediment with a micromanipulator (PyroScience,

139   Germany), in steps of 100-200 µm, depending on the oxygen concentration. Three O_2 profiles were measured in

140   one sediment core of each station. The O_2 profiles were measured directly after core retrieval, i.e. within 10 – 15

141   minutes.

142   **Sediment samples**

143   The surface sediment samples (first 1 cm) of the cruises HE 383 (06/07-2012) and HE 447 (06-2015) were

144   analyzed for total carbon and total nitrogen contents with an elemental analyzer (Carlo Erba NA 1500) The total

145   organic carbon content was analyzed after removal of inorganic carbon using 1 mol L^{-1} hydrochloric acid. The

146   standard deviation of sediment samples was better than 0.6 % for C_{org} and 0.08 % for N determination.

147   Permeabilty and porosity of the sediments were conducted with sediments from the cruise He-471, the methods

148   were described in detail elsewhere (Neumann, 2016).

149   **Dissolved inorganic nitrogen concentrations**

150   NO_x, NO_2^- and NH_4^+ concentrations of the water column samples were determined in replicate with a continuous

151   flow analyzer (AA3, Seal Analytics, Germany) according to standard colorimetric techniques (NO_x, NO_2:

152   (Grasshoff et al., 1999), NH_4^+: (Kérouel and Aminot, 1997)). NO_3^- concentration was calculated by difference

153   between NO_x and NO_2^-. Based on replicate analyses, measurement precision for NO_x and NO_2^- was better than 0.1

154   μmol L^{-1} and better than 0.2 μmol L^{-1} for NH_4^+.

155   Water samples from core incubations were analyzed in duplicate for concentration of NH_4^+, NO_2^- and NO_3^- using

156   a multimode microplate reader Infinite F200 Pro and standard colorimetric techniques (Grasshoff et al., 1999) at

157   the ZMT, Bremen. The standard deviations were <1 μmol L^{-1} for NO_3^-, <0.2 μmol L^{-1} for NO_2^- and <0.5 μmol L^{-1}

158   ^{1} for NH_4^+.

159   **Nitrogen isotope analyses**

160   The nitrogen isotope ratios of NO_3^- were determined via the denitrifier method (Casciotti et al., 2002; Sigman et

161   al., 2001). This method is based on the mass spectrometric measurement of isotopic ratios of N_2O produced by the

162   bacterium *Pseudomonas aureofaciens*. Briefly, 20 nmoles of sample NO_3^- were injected in a 20 ml vial containing

163   MilliQ. Two international standards were used (IAEA-NO_3^- $\delta^{15}N$ = +4.7 ‰, USGS-34 $\delta^{15}N$ = -1.8 ‰) for a

164   regression-based correction of isotope values. For further quality assurance, an internal standard was measured

165   with each batch of samples. The standard deviation for $\delta^{15}N$ was better than <0.2 ‰

166   For ammonium isotope measurements, nitrite was removed by reduction with sulfamic acid (Granger and Sigman,

167   2009) before NH_4^+ was chemically oxidized to NO_2^- by hypobromite at pH ~12 and then reduced to N_2O using

168   sodium azide (Zhang et al., 2007). 10 nmol of NH_4^+ were injected, and all samples with [NH_4^+] >1 μmol L^{-1} were

169   analyzed. For the calibration of the ammonium isotopes, we used three international standards (IAEA-N1 $\delta^{15}N$ =

170   +0.4 ‰, USGS 25 $\delta^{15}N$ = -30.4 ‰, USGS 26 $\delta^{15}N$ = +53.7 ‰). The standard deviations were better than 1 ‰.

171   N_2O produced either by the denitrifier method or the chemical conversion of ammonium was analysed with a

172   GasBench II, coupled to an isotope ratio mass spectrometer (Delta Plus XP, Thermo Fisher Scientific).

173   **2.4. Rates and fluxes calculation for respiration, ammonification, nitrification and denitrification rates in**

174   **core incubations**

175   *Benthic fluxes*

176   Oxygen consumption, net ammonification, net nitrification and denitrification were calculated based on

177   concentration changes in the sediment incubations. The respective benthic fluxes were calculated as follows:

178   r_{net} = d(C)*V/d(t)*A [mmol N m^{-2} d^{-1}]   (1)

179 where d(C) is the oxygen, nutrient or the nitrogen (N_2) concentration at the start and at the end of the experiment,

180 V is the volume of the overlying water, d(t) is the incubation time and A is the surface area of the sediment..

181 Positive fluxes (outflow concentrations above inflow concentrations) imply net production in the sediment.

182 *Gross rates of ammonification and nitrification*

183 Gross rates of ammonification and nitrification (r_{gross}) were calculated based on ^{15}N isotope dilution (Koike and

184 Hattori, 1978; Nishio et al., 2001). For example, ammonification rates are calculated based on $^{15}NH_4^+$ additions,

185 nitrification rates are based on $^{15}NO_3^-$ additions (Fig. 2) :

186 $r_{gross} = [\ln(f^{15}N_{end}/f^{15}N_{start})]/(\ln(C_{end}/C_{start}))*(C_{start}-C_{end}/t)*(V/A*\Delta t)$ (2)

187 where C_{start} is the initial NH_4^+ or NO_3^- concentration, C_{end} is the concentration at time t, and $f^{15}N_{start}$ and $f^{15}N_{end}$

188 represent ^{15}N atom% excess (Brase et al., 2018), V is the volume of the overlying water and A is the surface area

189 of the sediment. All rates are given in mmol N m^{-2} d^{-1}.

190 **3 Results**

191 *Ammonification*

192 We measured gross ammonification rates with the isotope dilution method using $^{15}NH_4^+$ as tracer, and measured

193 net ammonium fluxes with the flux method. The highest net ammonium flux and gross ammonification rates were

194 measured in the impermeable, organic-rich sediment at station NOAH-C (6.6 ±1.4 mmol N m^{-2} d^{-1} and 9.5 mmol

195 N m^2 d^{-1} for net flux and gross ammonification, respectively).

196 The lowest net ammonium fluxes were measured in the semi-impermeable sediment at station NOAH-D (0.5 ±

197 0.1 mmol N m^{-2} d^{-1}). The lowest gross ammonification rate was measured at the permeable sediment station

198 NOAH-A (2.1 ± 0.3 mmol N m^{-2} d^{-1}). The impermeable sediment station NOAH-C had the highest net ammonium

199 fluxes (6.6 ±1.4 mmol N m^{-2} d^{-1}) and gross ammonification rates (9.5 mmol m^{-2} d^{-1}). Net and gross ammonification

200 rates are significantly correlated (r^2=0.55; see electronical supplemental).

201 *Nitrification*

202 As for the ammonification, we measured gross nitrification rates by means of the stable isotope dilution method

203 with $^{15}NO_3^-$ as tracer, and net nitrate fluxes employing the flux method. Net fluxes and gross nitrification rates

204 varied significantly between stations. Net nitrate fluxes were highest at station NOAH-C and at station NOAH-E

205 with 1.1 ± 0.5 mmol N m^{-2} d^{-1} and 1.2 ±0.5 mmol N m^{-2} d^{-1}, respectively (Fig. 3, Fig. 5). Gross nitrification rates

206 were highest at NOAH-C (2.1 ± 0.1 mmol N m^{-2} d^{-1}). The lowest rates of net nitrate flux (0.3 ± 0.3 mmol N m^{-2} d^{-}

207 ^{1}) and gross nitrification (1.2 ± 0.0 mmol m^{-2} d^{-1}) were observed in the permeable sediment at station NOAH-A.

208 Net and gross nitrification rates are closely correlated (r^2=0.87; Fig. 3) with net nitrate fluxes being systematically

209 lower than gross nitrification rates.

Denitrification

Unlike to ammonification and nitrification, we were not able to make use of the stable isotope tracers to evaluate N_2 production rates with a stable isotope technique because the requirements for the Isotope Pairing method (Rysgaard-Petersen et al., 1996) were not met because the labeled $^{15}NO_3^-$ in the overlying water is too low to measure any $^{15}N-N_2$ species. Our N_2 production estimates are thus limited to the flux method. The observed average denitrification rates ranged from 1.3 ± 1.1 mmol N m^{-2} d^{-1} to 1.9 ± 0.8 mmol N m^{-2} d^{-1} N m^{-2} d^{-1} (Fig. 5) and did not vary significantly between stations.

Sedimentary organic matter descriptions

The data show a clear correlation between sediment type and organic carbon and nitrogen content. Clay and silty sediment (NOAH-C) had the highest organic carbon (0.73 %) and nitrogen (0.10 %) concentrations (Tab. 2). Medium sand station (NOAH-A) had the lowest C_{org} (0.03 to 0.04 %) and total nitrogen (<0.01 to 0.01 %) concentrations. This trend does probably not apply to NOAH-E since the samples for C / N analyses were retrieved prior to the abrupt emergence of a large pockmark field at this station (Krämer et al. 2017) while the sediment cores for the incubations were retrieved after the emergence of the pockmarks. The large scale sediment resuspension event resulted in numerous newly formed depressions with increased sedimentation of organic material.

4 Discussion

4.1 Magnitude and relevance of ammonification

A principal goal of this study was to assess the role of ammonification in the nitrogen cycle of the German Bight. Ammonification releases NH_4^+ during the decomposition of organic matter and resupplies the water-column inventory of reactive nitrogen. The quantification of ammonification rates is challenging, because ammonium is readily assimilated by primary producers or is rapidly nitrified, causing low ammonium concentrations and necessitating to use the isotope dilution method.

This study represents direct measured gross ammonification rates across typical sediment types of the North Sea, covering a large range from 1.9 to 9.5 mmol N m^{-2} d^{-1}: Ammonification rates were mainly governed by sediment texture and organic matter content. The impermeable muddy sediment at station NOAH-C with high C_{org} and TN content (0.73 % and 0.10 %, respectively, Tab. 2) had highest gross and net ammonification rates. This is line with other studies showing enhanced ammonium release in muddy coastal sediments (e.g. Caffrey, 1995).

239 The sandy sediments at sites NOAH-A, NOAH-D and NOAH-E exhibited significantly lower gross

240 ammonification rates. This reflects the lower sediment organic matter content in these sandy sediments expressed

241 in C_{org} (0.03 – 0.04 %) and N (0.01 – <0.01 %) concentrations (Caffrey, 1995), Tab. 2).

242 It is striking, though, that net and gross ammonification in the sandy sediment at station NOAH-E was clearly

243 elevated compared to the other sandy stations NOAH-A and NOAH-D. There are two possible explanations for

244 this enhanced ammonium production: (1) enhanced supply of organic matter to the sediment surface or (2) effects

245 bioirrigation and bioturbation.

246 Station NOAH-E is located inside a pockmark field that had developed relatively recently, between July and

247 November 2015 (Krämer et al., 2017). Our assessment of C and N content is based on samples that were taken

248 prior to the pockmark formation in 2012 and 2015 (https://doi.org/10.1594/PANGAEA.883199). The sediment

249 samples during the cruise (He-471) in 2016 were taken from the depression inside an individual pockmark, which

250 was about ~0.2 deeper than the surrounding sediment (Krämer et al., 2017). We assume that organic matter from

251 the water column accumulated in these transient structures, and that the organic carbon and nitrogen content thus

252 was elevated. A transient change in surface sediment composition, which is not captured by our compositional

253 data, may thus have caused the enhanced ammonification rate.

254 An alternative explanation is an elevation of ammonium fluxes from the sediment due to sediment reworking. In

255 the sediment incubations, we found a high benthic activity of *Spiophanes bombyx* and *Phoronis sp.*. Both benthic

256 organisms can increase the nutrient fluxes from the sediment to the bottom water, the oxygen penetration depth,

257 and, in turn, organic matter degradation in the oxic zone (Aller, 1988).

258 Under completely oxic conditions, the ratio of NH_4^+ release and O_2 consumption in the entire study area should

259 approximate Redfield ratios of about 1:8.6 (Thibodeau et al., 2010). Such ratios were observed at the semi-

260 permeable station NOAH-D, the permeable station NOAH-A (Fig. 2), and at station NOAH-E, suggesting that in

261 these cores most of the organic matter was degraded under oxic conditions. At station NOAH-C, however, the

262 $N:O_2$ ratio was clearly elevated above the Redfield ratio. While this finding is based on an individual assessment,

263 it appears plausible: We presume that the enhanced production of ammonium relative to O_2 consumption reflects

264 the importance of anoxic ammonium generation, i.e., during methanogenesis or sulfate reduction (e.g. Jorgensen,

265 1982). This is quite likely at station NOAH-C, where oxygen penetration depth in the impermeable, organic-rich

266 sediment is lowest, and where increasing NH_4^+ concentrations with depth indicate decomposition or organic matter

267 in the absence of free oxygen (Hartmann et al., 1973).

268 **4.2 Ammonification coupled to denitrification by nitrification**

269 Based on the interpolation of gross rates of ammonification, it is evident that ammonification contributes

270 significantly to nutrient regeneration in the German Bight. However, there is a clear difference between gross and

271 net ammonification rates, suggesting that ammonium is taken up, either by assimilation or nitrification. In dark

272 sediments, where phototrophic organisms are light limited, we presume that nitrification is likely the more

273 important process (Dähnke et al., 2012).

274 Nitrification produces NO_3^-, which represents the largest DIN pool in the water column of the North Sea and is the

275 substrate for denitrification, and thus the link to an ultimate removal of fixed nitrogen from the water column.

276 We observed gross nitrification rates at all four stations ranging from 1.2 ± 0.0 mmol N m^{-2} d^{-1} at the sandy station

277 NOAH-A, to 1.3 mmol N m^{-2} d^{-1} in the moderately permeable sediment at NOAH-D and to 2.1 ± 0.1 mmol N m^{-2}

278 d^{-1} in the impermeable sediment at station NOAH-C (Fig. 3, Fig. 5). Gross nitrification at the impermeable

279 sediment station NOAH-C accounted for around 22.2 % (±0.7 %), around 38.5 % at the semi-permeable station

280 (NOAH-D) and around 50.6 % (±15.8 %) at the permeable sediment stations of total DIN flux to the bottom water.

281 Overall, nitrification is in the same range as reported by Marchant et al. (2016) in sandy sediment near Helgoland

282 (0.2 to 3.0 mmol m^{-2} d^{-1}; Tab. 1). Highest nitrate fluxes from the sediment and gross nitrification rates were

283 observed at the impermeable station NOAH-C and at station NOAH-E, where pockmark structure and organic

284 matter accumulation might have affected benthic nutrient fluxes (see section 4.1).

285 Lowest gross nitrification rates and nitrate fluxes are found at the permeable station NOAH-A, but apart from this,

286 we do not see a clear correlation of nitrification and permeability in our study. Nonetheless, nitrification rates are

287 lowest at Station NOAH-A, where oxygen penetration depth is highest, and the sediment has low organic matter

288 content (Tab. 2). A high oxygen penetration depth can support nitrification, but it is in this case obviously substrate

289 limited due to low organic matter content, which limits ammonification. Oxygen penetration can enhance

290 nitrification at greater depth, but can, on the other hand, also increase diffusion limitation (Alkhatib et al., 2012).

291 Due to this dual control of nitrification by OPD on the one hand and substrate availability on the other, the

292 individual correlations between C_{org} or TN and nitrification are relatively weak. Generally, organic matter

293 deposition in the sediment supports higher ammonification rates, which in turn enhance nitrification under oxic

294 conditions (Henriksen and Kemp, 1988; Rysgaard et al., 1996). Consequently, nitrification is affected by the NH_4^+

295 pool in the sediment, temperature, salinity and O_2 (e.g. Sanders, 2018).

296 This interplay of factors is mirrored in a clear and statistically significant (a=0.05) correlation of gross nitrification

297 and gross ammonification rates ($r^2 = 0.92$). Overall, the gross NO_3^- production (1.2 to 2.1 mmol m^{-2} d^{-1}) was small

298 relative to ammonification rates (1.9 to 9.5 mmol N m^{-2} d^{-1}). We find that nitrification is governed by a complex

299 interplay of variables such as ammonification rate, permeability, organic matter availability and oxygen

300 penetration depth, and is likely difficult to predict based on one of these factors alone. Generally, organic matter

301 deposition in the sediment supports higher ammonification rates, which in turn enhance nitrification under oxic

302 conditions (Henriksen and Kemp, 1988; Rysgaard et al., 1996). In our setting, this is reflected in a clear correlation

303 of gross rates of ammonification and nitrification.

304 **4.3 Denitrification**

305 Denitrification, the reduction of NO_3^- to gaseous N_2, reduces the pool of bioavailable N, and is therefore very

306 relevant in eutrophic coastal areas such as the southern North Sea. In our study, the measured denitrification rates

307 ranged from 1.3 to 1.9 mmol N m^{-2} d^{-1} (Fig. 5). This estimate is on the higher end of previous measurements from

308 sites in the German Bight (Deek et al., 2013; Marchant et al., 2016) (Tab. 1), but generally fits with previous

309 observations. We assume that the rates in our study are elevated because sampling took place after the spring

310 phytoplankton bloom, and not all organic matter that had been deposited at the sediment surface had been

311 remineralized. Such a decoupling of water column production and sedimentary denitrification has been observed

312 before in stratified water masses of the Baltic Sea (Hellemann et al., 2017). Even though our study was designed

313 to cover diverse sediment types, and thus allow for an improved extrapolation of rates to the total German Bight

314 area, this highlights the heterogeneity of sediments, and points out that the sampling season can have a marked

315 effect on measured rates. Therefore, follow-up experiments should try to cover the seasonality as much as possible

316 to improve estimates of denitrification in the German Bight area.

317 Important seasonal effects on denitrification can be attributed to variations in oxygen supply, changing bottom

318 water NO_3^- concentration and organic carbon content in the sediment (Deek et al., 2013). In our study, the bottom

319 water nitrate concentration is too low (<0.5 to 4.5 µmol L^{-1}) to sustain the observed denitrification rates, and thus

320 the major nitrate source fueling the observed denitrification must be coupled nitrification-denitrification fueled by

321 mineralization of sedimentary organic material. This is reflected in a strong correlation between gross nitrification

322 and denitrification rates ($r^2 = 0.85$).

323 In our study, we find that this coupled nitrification-denitrification determines the total N flux. Denitrification

324 essentially removes, within the given uncertainties (Fig. 5) all nitrate produced by nitrification at study sites

325 NOAH-A and NOAH-D. At stations NOAH-C and NOAH-E, where we assume a (possibly transient in case of

326 NOAH-E) accumulation of organic matter, nitrification rates are enhanced, and a substantial amount of freshly

327 produced nitrate is released to the water column.

328 In comparison to the supply of mineralized N (i.e., gross ammonification) denitrification accounts for ~20 % (1.9

329 mmol N m^{-2} d^{-1} / 9.5 mmol N m^{-2} d^{-1}) at the impermeable sediment station NOAH-C, ~39 % (1.3 mmol N m^{-2} d^{-1}

330 / 3.3 mmol N m^{-2} d^{-1}) at the semi-permeable sediment station NOAH-D and ~ 62 % (1.3 mmol N m^{-2} d^{-1} / 2.1

331   mmol N m^{-2} d^{-1}) at permeable sediment stations (NOAH-A). As discussed above, this trend does not hold for the

332   less representative station NOAH-E due to the transient formation of numerous pockmarks.

333   **4.4 Significance of benthic N-recycling**

334   Our study covers the most sediment types across the German Bight, but is based on core incubations and therefore

335   potentially underestimates advective processes. In a recent study by Neumann et al. (2017), the authors used NO$_3^-$

336   pore water profiles to calculate the NO$_3^-$ consumption rates across a similar range of North Sea sediments. They

337   extrapolated their nitrate consumption rates to the entire area of the German Bight based on a permeability

338   classification of sediments. They propose that ~24 % of sediments in the southern North Sea (German Bight) are

339   impermeable sediments (12,200 km^{-2}), ~39 % are moderately permeable sediments (19,600 km^{-2}) and ~37 %

340   (18,800 km^{-2}) are permeable sediments. They estimated that permeable sediment were the most efficient NO$_3^-$ sink

341   accounting for up to 90 % of the total benthic NO$_3^-$ consumption. In our assessment, which better represents the

342   role of nitrification, we arrive at a somewhat lower contribution of ~68 % of total denitrification occurring in

343   moderately permeable and permeable sediments. Based solely on our data, we estimate a total nitrogen removal

344   of ~1030 t N d^{-1} in our study area, which corresponds to an average N$_2$ flux of approximately 1.5 mmol N m^{-2} d^{-1}.

345   This daily N$_2$ production during late summer equals the total N discharge (~1.000 t N d^{-1}) by the main rivers Maas,

346   Rhine, North-Sea Canal, Ems, Weser and Elbe (Pätsch and Lenhart, 2004), and, as such, underscores the role of

347   coastal sediments to counteract the eutrophication in the North Sea.

348   Our assessment, however, does reflect the impact of only diffusive transport and faunal activity while not

349   accounting for advective fluxes. Based on the same data set of permeability for classification of different sediment

350   types that Neumann et al. (2017) used, we will merge our dataset with the results of Neumann et al. (in preparation)

351   to arrive at an improved estimate of sediment denitrification that includes benthic nitrification as a nitrate source.

352   In the following, we aim to put our estimates of N-transition rates into perspective by setting an upper limit of N

353   turnover based on primary production since N cycling is linked to organic carbon availability, which is ultimately

354   provided by pelagic primary production. For the freshwater influenced regions of the German Bight, Capuzzo et

355   al. (2018) assume a C fixation of 1.05 g C m^{-2} d^{-1}. For an estimate of the maximum N transition rate we assume

356   that 10 % of the fixed C is processed in the sediment (Heip et al., 1995) and that all carbon is remineralized in the

357   sediment in pace with N turnover. Based on Redfield stoichiometry (~12 g / mol C, ~14 g / mol N), average C

358   fixation translates to [1.05 g * 10 % / 12 C * 14N =] 0.123 mg N that is removed per m^{-2} and day, or 9 mmol N m^{-}

359   ^{2} d^{-1}, respectively. This sets an upper limit to the N turnover rate and compares well with the observed

360   ammonification rate in impermeable sediment at NOAH-C (9.5 mmol NH$_4^+$ m^{-2} d^{-1}, Figure 5). The ammonification

361   rates at the sandy stations are substantially lower, which certainly reflects that sandy sediments are frequently

362 resuspended and organic particles are resuspended and degraded in the water column. For a second line of

363 argument, we consider the annual nitrate budget of the southern North Sea (Hydes et al. 1999, van Beusekom et

364 al. 1999) with an annual average denitrification rate of 0.7 mmol N m^{-2} d^{-1}. This value agrees well with the average

365 gap of 0.5 mmol N m^{-2} d^{-1} between gross nitrification and actual nitrate flux (Figure 4), which we attribute to

366 denitrification. Both rates, the budget-based estimate and the nitrification gap are in the lower range of our

367 measured N_2 fluxes of 0.3 to 2.9 mmol N m^{-1} d^{-1} (Tab. 1, Fig. 5). For a third line of argument, we employ the

368 approach of Seitzinger and Giblin (1996) to link benthic respiration and denitrification directly to the pelagic

369 primary production. By employing their formulas and using the primary production rates by Capuzzo et al. (2018),

370 the annual average of the sediment oxygen demand would be 14.3 mmol O_2 m^{-2} d^{-1} (1.05 g C d^{-1} m^{-2} = 87.5 mmol

371 C d^{-1} m^{-2}), which corresponds to a benthic denitrification rate of 3.3 mmol N m^{-2} d^{-1}. Since the annual average of

372 actually measured oxygen fluxes are close to this estimate (15.4 ± 12.9 mmol O_2 m^{-2} d^{-1}, N=175) (Neumann et al.,

373 in preparation), we are confident that our denitrification estimates of up to 2.9 mmol N m^{-2} d^{-1} are reasonable.

374 However, with the multitude of our approaches yielding quite a span of plausible denitrification estimates the

375 question emerges which of the figures in the range of 0.5 to 3.3 mmol N m^{-1} d^{-1} is actually the true value for the

376 average denitrification rate. One major reason for this level of uncertainty is the fact that the local sediment

377 properties with regard to macrofauna composition and organic matter content varied considerably within each

378 station, which is reflected e.g. in the variability of oxygen consumption rates (see electronic supplemental). Since

379 we were restricted to 4 cores per station in total, and just 2 cores for labelling with $^{15}NH_4^+$ and $^{15}NO_3^-$, respectively,

380 the inevitable spatial heterogeneity introduced a substantial degree of random error. Additionally, the preceding

381 results we used above to evaluate our observations are certainly likewise based on imperfect data, which results in

382 uncertainty on that side. In summary, our limited set of new observations is not sufficiently large to favor one of

383 the preceding denitrification estimates. At least, the average of all our N_2 measurements of 1.5 ± 0.9 mmol N m^{-2}

384 d^{-1} (N=13) falls right in the center of the interval of 0.5 to 3.3 mm and might represent our best estimate for an

385 average denitrification rate in late summer. The remaining fraction of the initial ammonification is recycled back

386 into the water column as DIN, which accounts for 69 ± 18 % (N=12) of the total benthic N flux (N_2 + DIN).

387 Since benthic N recycling substantially restocks the pelagic N inventory, we further assessed the contribution of

388 benthic N recycling by comparing the benthic DIN (ammonium + nitrite + nitrate) fluxes with the inventory of

389 DIN below the thermocline. Assuming steady state, we find a rapid turnover of sediment-derived DIN at NOAH-

390 C and NOAH-E, in the range of 1-3 days (Tab. 3). This implies that even below the thermocline, DIN derived by

391 the sediment is rapidly assimilated by phytoplankton. Previous publications showed that primary production below

392 the thermocline contributes ~ 37 % to total primary production in the North Sea (van Leeuwen et al., 2013).

393 Assuming Redfield stoichiometry and an average primary production of 1.05 g C m^{-2} d^{-1}, benthic DIN fluxes in

394 our measurements can support a primary production of about 6.2 to 51.4 mmol C m^{-2} d^{-1} or 74 – 617 mg C m^{-2}

395 day^{-1}. This is within the range of previously observed and modeled primary production rates in the North Sea

396 during summer (e.g. van Leeuwen et al., 2013). We further estimate that depending on the thickness of the bottom

397 water layer below the thermocline, benthic N fluxes during the sampling time supported between 7.1 ± 2.6 % (38

398 m bottom water layer) and 58.7 ±10.6 % (10 m bottom water layer) of the annual average of primary production

399 (Tab. 3). This dependence of relative sediment contribution on water depth has been observed previously for

400 respiration processes (Heip et al., 1995). Our data also match the calculation of Blackburn and Henriksen (1983)

401 for Danish sediments, where N fluxes could support 30 to 83 % of the nitrogen requirement of the planktonic

402 primary producers (Blackburn and Henriksen, 1983).

403

404 **5 Summary and concluding remarks**

405 We evaluated a range of sedimentary nitrogen turnover pathways and found that ammonification in sediments is

406 an important N-source for primary production in the water column of the southeastern North Sea during summer.

407 Depending on water depth, 7.1 to 58.7 % of the estimated water column primary production is fueled by

408 sedimentary N release. Nitrification act as the main sinks of NH$_4^+$ mineralized from sedimentary organic matter.

409 Ultimately, the main factors governing nitrification are organic matter content / ammonification and oxygen

410 penetration depth in the sediment. The share of newly produced NO$_3^-$ reduced to N$_2$ amounts to two thirds of NO$_3^-$

411 in permeable sediments, to nearly one half in moderately permeable sediment, and to one third in impermeable

412 sediments. We further showed that moderately permeable and permeable sediments account for up to ~80 % of

413 the total benthic N$_2$ production (~1030 t N d^{-1}) in the southern North Sea (German Bight) during the peak of benthic

414 activity in late summer. Only then, benthic N$_2$ production can compensate the annually averaged daily N input by

415 the main rivers (e.g. Elbe, Ems, Rhine, Weser) discharging into the southern North Sea (~1.000 t N d^{-1}). Thus

416 impermeable sediments act as an important N source for primary producers, whereas moderately permeable and

417 permeable sediments comprise a main reactive N sink counteracting eutrophication in the North Sea. Seasonal and

418 spatial variabilities, especially from nearshore to offshore, should be evaluated in future studies.

419

420 **Acknowledgements**

421 We thank the captain and the crew of *R/V Heincke* for their support during the sampling campaigns. M. Birkicht

422 from the Leibniz Centre for Tropical Marine Research (ZMT) in Bremen is gratefully acknowledged for his

423   assistance with nutrient measurements. We further thank E. Logemann for the analysis of macrobenthos. We also

424   gratefully thank the two anonymous reviewers for comments that helped to greatly improve this manuscript.

References

Alkhatib, M., Lehmann, M. F., and del Giorgio, P. A.: The nitrogen isotope effect of benthic remineralization-nitrification-denitrification coupling in an estuarine environment, Biogeosciences, 9, 1633-1646, 2012.

Aller, R. C.: Benthic Fauna and Biogeochemical Processes in Marine Sediments: The Role of Burrows Structures. In: Nitrogen cycling in Coastal Marine Environments, Blackburn, T. H. and Sørensen, J. (Eds.), Scope, Chichester, 1988.

Bale, N. J., Villanueva, L., Fan, H., Stal, L. J., Hopmans, E. C., Schouten, S., and Sinninghe Damste, J. S.: Occurrence and activity of anammox bacteria in surface sediments of the southern North Sea, FEMS Microbiol Ecol, 89, 99-110, 2014.

Blackburn, T. H. and Henriksen, K.: Nitrogen cycling in different types of sediments from Danish waters, Limnology and Oceanography, 28, 477-493, 1983.

Brase, L., Sanders, T., and Daehnke, K.: Anthropogenic changes of nitrogen loads in a small river: external nutrient sources vs. internal turnover processes, Isotopes in Environmental and Health Studies, 54, 168-184, 2018.

Burger, M. and Jackson, L. E.: Microbial immobilization of ammonium and nitrate in relation to ammonification and nitrification rates in organic and conventional cropping systems, Soil Biology and Biochemistry, 35, 29-36, 2003.

Cadée, G. C. and Hegemann, J.: Phytoplankton in the Marsdiep at the end of the 20th century; 30 years monitoring biomass, primary production, and Phaeocystis blooms, Journal of Sea Research, 48, 97-110, 2002.

Caffrey, J. M.: Spatial and Seasonal Patterns in Sediment Nitrogen Remineralization and Ammonium Concentrations in San Francisco Ba,y California, Estuarine, Coastal and Shelf Science, 18, 219-233, 1995.

Capuzzo, E., Lynam, C. P., Barry, J., Stephens, D., Forster, R. M., Greenwood, N., McQuatters-Gollop, A., Silva, T., van Leeuwen, S. M., and Engelhard, G. H.: A decline in primary production in the North Sea over 25 years, associated with reductions in zooplankton abundance and fish stock recruitment, Glob Chang Biol, 24, e352-e364, 2018.

Casciotti, K. L.: Nitrogen and Oxygen Isotopic Studies of the Marine Nitrogen Cycle, Ann Rev Mar Sci, 8, 379-407, 2016.

Casciotti, K. L., Sigman, D. M., Hastings, M. G., Böhlke, J. K., and Hilkert, A.: Measurement of the oxygen isotopic composition of nitrate in seawater and freshwater using the denitrifier method, Anal. Chem., 74, 4905-4912, 2002.

Dähnke K., Moneta A., Veuger B., Soetaert K., Middelburg J.J.: Balance of assimilative and dissimilative nitrogen processes in a diatom-rich tidal flat sediment. Biogeosciences. 2012;9:4059-70, 2012.

Deek, A., Dähnke, K., van Beusekom, J., Meyer, S., Voss, M., and Emeis, K.: N_2 fluxes in sediments of the Elbe Estuary and adjacent coastal zones, Marine Ecology Progress Series, 493, 9-21, 2013.

Deek, A., Emeis, K., and van Beusekom, J.: Nitrogen removal in coastal sediments of the German Wadden Sea, Biogeochemistry, 108, 467-483, 2011.

Emeis, K.-C., van Beusekom, J., Callies, U., Ebinghaus, R., Kannen, A., Kraus, G., Kröncke, I., Lenhart, H., Lorkowski, I., Matthias, V., Möllmann, C., Pätsch, J., Scharfe, M., Thomas, H., Weisse, R., and Zorita, E.: The North Sea — A shelf sea in the Anthropocene, Journal of Marine Systems, 141, 18-33, 2015.

Granger, J. and Sigman, D. M.: Removal of nitrite with sulfamic acid for nitrate N and O isotope analysis with the denitrifier method, Rapid Commun Mass Spectrom, 23, 3753-3762, 2009.

Grasshoff, K., Kremling, K., and Ehrhardt, M.: Methods of Seawater Analysis, Wiley-VCH, Weinheim, 1999.

Hartmann, M., Müller, P., Suess, E., and Van der Weijden, C. H.: Oxidation of organic matter in recent marine sediments, Meteor Forschungs-Ergebnisse, Reihe C, 74-86, 1973.

475 Heip, C. H. R., Goosen, N. K., Herman, P. M. J., Kromkamp, J., Middelburg, J. J., and Soetaert, K.:
476 Production and consumption of biological particles in temperate tidal etuaries, Oceanography and
477 Marine Biology, 33, 1-149, 1995.
478 Hellemann, D., Tallberg, P. and Hietanen, S.: Benthic N_2 production rates, Si cycling and
479 environmental characteristics from the Öre estuary on the Swedish coast,Marine Ecology Progress
480 Series, 583, 63-80, 2017.
481 Henriksen, K. and Kemp, W. M.: Nitrification in Estuarine and Coastal Marine Sediments. In: Nitrogen
482 Cycling in Coastal Marine Environments, Blackburn, T. H. and Sorensen, J. (Eds.), John Wiley & Sons
483 Ltd, SCOPE, 1988.
484 Hickel, W., Mangelsdorf, P., and Berg, J.: The human impact in the German Bight: Eutrophication
485 during three decades (1962-1991), Helgoländer Meeresun, 47, 243-263, 1993.
486 Hydes, D. J., Kelly-Gerreyn, B. A., Le Gall, A. C., and Proctor, R.: The balance of supply of nutrients and
487 demands of biological production and denitrification in a temperate latitude shelf sea – a treatment
488 of the southern North Sea as an extended estuary, Marine Chemistry, 68, 117-131, 1999.
489 Jensen, K. M., Jensen, M. H., and Kristensen, E.: Nitrification and denitrification in Wadden Sea
490 sediments (Konigshafen, Island of Sylt, Germany) as measured by nitrogen isotope pairing and
491 isotope dilution, 11, 181-191, 1996.
492 Jorgensen, B. B.: Mineralization of organic matter in the sea bed-the role of sulphate reduction,
493 Nature, 296, 643-645, 1982.
494 Jorgensen, B. B.: Processes at the sediment-water interface. In: The Major Biogeochemical Cycles and
495 Their Interactions, Bolin, B. and Cook, R. B. (Eds.), John Wiley, New York, 1983.
496 Kana, T. M., Darkangelo, C., Hunt, M. D., Oldham, J. B., Bennett, G. E., and Cornwell, J. C.: Membrane
497 Inlet Mass Spectrometer for Rapid High-Precision Determination of N_2, O_2, and Ar in Environmental
498 Water Samples.pdf>, Analytical Chemistry, 66, 4166-4170, 1994.
499 Kérouel, R. and Aminot, A.: Fluorimethic determination of ammonia in sea and estuarine water by
500 direct segmented flow analysis. , Marine Chemistry, 57, 265-275, 1997.
501 Koike, I. and Hattori, A.: Simultaneous determinations of nitrification and nitrate reduction in coastal
502 sediments by a ^{15}N dilution technique, Appl Environ Microbiol, 35, 853-857, 1978.
503 Krämer, K., Holler, P., Herbst, G., Bratek, A., Ahmerkamp, S., Neumann, A., Bartholoma, A., van
504 Beusekom, J. E. E., Holtappels, M., and Winter, C.: Abrupt emergence of a large pockmark field in the
505 German Bight, southeastern North Sea, Sci Rep, 7, 5150, 2017.
506 Lenhart, H. J. and Pohlmann, T.: The ICES-boxes approach in relation to results of a North Sea
507 circulation model, Tellus A: Dynamic Meteorology and Oceanography, 49, 139-160, 1997.
508 Lohse, L., Malschaert, J. F. P., Slomp, C. P., Helder, W., and van Raaphorst, W.: Nitrogen cycling in the
509 North Sea sediments: interaction of denitrification and nitrification of offshore and coastal areas,
510 Marine Ecology Progress Series, 101, 283-296, 1993.
511 LOICZ: Land-Ocean Interactions in the Coastal Zone, 1995.
512 Los, F. J., Troost, T. A., and Van Beek, J. K. L.: Finding the optimal reduction to meet all targets—
513 Applying Linear Programming with a nutrient tracer model of the North Sea, Journal of Marine
514 Systems, 131, 91-101, 2014.
515 Marchant, H. K., Holtappels, M., Lavik, G., Ahmerkamp, S., Winter, C., and Kuypers, M. M. M.:
516 Coupled nitrification-denitrification leads to extensive N loss in subtidal permeable sediments,
517 Limnology and Oceanography, 61, 1033-1048, 2016.
518 Neubacher, E. C., Parker, R. E., and Trimmer, M.: Short-term hypoxia alters the balance of the
519 nitrogen cycle in coastal sediments, Limnology and Oceanography, 56, 651-665, 2011.
520 Neumann, A.: Elimination of reactive nitrogen in continental shelf sediments measured by
521 membrane inlet mass spectrometry., PhD, Department Geowissenschaften, Universität Hamburg,
522 Hamburg, 2012.
523 Neumann, A., van Beusekom, J. E. E., Eisele, A., Emeis, K.-C., Friedrich, J., Kröncke, I., Logemann, E. L.,
524 Meyer, J., Naderipour, C., Schückel, U., Wrede, A., and Zettler, M.: Elucidating the impact of
525 macrozoobenthos on the seasonal and spatial variability of benthic fluxes of nutrients and oxygen in
526 the southern North Sea, in preparation. in preparation.

527 Neumann A., Möbius J., Hass H. C., Puls W., Friedrich J.: Empirical model to estimate permeability of
528 surface sediment in the German Bight (North Sea). Journal of Sea Research 127, 36-45, 2016.
529 Neumann, A., van Beusekom, J. E. E., Holtappels, M., and Emeis, K.-C.: Nitrate consumption in
530 sediments of the German Bight (North Sea), Journal of Sea Research, 127, 26-35, 2017.
531 Nishio, T., Komada, M., Arao, T., and Kanamori, T.: Simultaneous determination of transformation
532 rates of nitrate in soil, Japan Agricultural Research Quarterly: JARQ, 35, 11-17, 2001.
533 OSPAR: Quality Status Report, London, 176 pp pp., 2010.
534 Pätsch, J. and Lenhart, H.-J.: Daily loads of nutrients, total alkalinity, dissolved inorganic carbon and
535 dissolved organic carbon of the European continental rivers for the years 1977-2002. In: Berichte aus
536 dem Zentrum für Meeres- und Klimaforschung, Reihe B: Ozeanographie, University of Hamburg,
537 Germany, 2004.
538 Redfield, A. C.: The biological control of chemical factors in the environment, American Scientist, 46,
539 205-221, 1958.
540 Rysgaard, S., Risgaard-Petersen, N., and Sloth, N. P.: Nitrification, denitrification and nitrate
541 ammonification in two coastal lagoons in Southern France, Hydrobiologia, 329, 133-141, 1996.
542 Sanders, T., Schöl, A., and Dähnke, K.: Hot spots of nitrification in the Elbe Estuary and their impact
543 on nitrate regeneration, Estuaries and Coasts, 41, 128-138, 2018.
544 Seitzinger, S. P. and Giblin, A. E.: Estimating denitrification in North Atlantic continental shelf
545 sediments, Biogeochemistry, 35, 235-260, 1996.
546 Sigman, D. M., Casciotti, K. L., Andreani, M., Barford, C., Galanter, M., and Böhlke, J. K.: A bacterial
547 method for the nitrogen isotopic analysis of nitrate in seawater and freshwater, Anal. Chem., 73,
548 4145-4153, 2001.
549 Thibodeau, B., Lehmann, M. F., Kowarzyk, J., Mucci, A., Gélinas, Y., Gilbert, D., Maranger, R., and
550 Alkhatib, M.: Benthic nutrient fluxes along the Laurentian Channel: Impacts on the N budget of the
551 St. Lawrence marine system, Estuarine, Coastal and Shelf Science, 90, 195-205, 2010.
552 Van Beusekom, J., Brockmann, U. H., Hesse, K.-J., Hickel, W., Poremba, K., and Tillmann, U.: The
553 importance of sediments in the transformation and turnover of nutrients and organic matter in the
554 Wadden Sea and German Bight, German Journal of Hydrography, 51, 245-266, 1999.
555 van Leeuwen, S. M., van der Molen, J., Ruardij, P., Fernand, L., and Jickells, T.: Modelling the
556 contribution of deep chlorophyll maxima to annual primary production in the North Sea,
557 Biogeochemistry, 113, 137-152, 2013.
558 von Westernhagen, H., Hickel, W., Bauerfeind, E., Niermann, U., and Kröncke, I.: Sources and effects
559 of oxygen deficiencies in the south-eastern North Sea, Ophelia, 26, 457-473, 1986.
560 Zhang, L., Altabet, M. A., Wu, T., and Hadas, O.: Sensitive Measurement of NH_4^+ $^{15}N/^{14}N$ ($\delta^{15}NH_4^+$) at
561 Natural Abundances Levels in Fresh and Saltwaters, Anal Chem, 79, 5297-5303, 2007.

562 **Table 1: Rates of nitrification, dissimilatory nitrogen reduction to ammonia (DNRA), anaerobic ammonia oxidation**
563 **(anammox) and denitrification (DNIT) (in µmol N m^{-2} d^{-1}) in the North Sea of other published data. Abbreviation of**
564 **methods: SIDM - sediment isotope dilution method; MABT - modified acetylene block technique; SSI - sediment slurry**
565 **incubations, PWMI – pore-water mean fitting, IPT - isotope-pairing technique.**

Location	Nitrification	DNRA	Anammox	DNIT rate / NO₃⁻ uptake	Sediment type	C_org	C:N	Sampling time	Method	Reference
	[µmol m^{-2} d^{-1}]				[-]	[% dry wt]	[atom]		[-]	
German Bight (North Sea)	1233 ± 12	N.D.	N.D.	1314 ± 1087	medium sand	0.03	<0.01	08./09.2016	SIDM	this study
	1739 ± 695	N.D.	N.D.	1355 ± 876		0.04	0.01			
	1271	N.D.	N.D.	1306 ± 1042	Fine sand	0.21	0.03			
	2069 ± 63	N.D.	N.D.	1915 ± 831	clay/silt	0.73	0.10			
Dutch Coast	N.D.	N.D.	0.0	N.D.	fine sand	0.03	N.D.	11.2010	SSI	(Bale et al., 2014)
			0.2					02.2011		
			1.3					05.2011		
			0.6					08.2011		
Oyster Ground	N.D.	N.D.	0.0	N.D.	muddy sand / clay / silt	0.30	N.D.	11.2010		
			2.3					02.2011		
			10.4					05.2011		
			12.8					08.2011		
North Dogger	N.D.	N.D.	0.0	N.D.	fine sand	0.03	N.D.	11.2010		
			0.8					02.2011		
			0.0					05.2011		
			1.1					08.2011		
Elbe Estuary / coastal zones	N.D.	N.D.	N.D.	771*	coarse sand	0.6	6.0	03.2009	IPT	(Deek et al., 2013)
				1215*		0.1	N.D.			
				3200*		0.1				
				864*		0.6	6.0			
				1425*		0.2		09.2009		
				47*		0.1	N.D.			
				140*		0.2				
Oyster Ground	288 ±144			12.0*	muddy sand	0.12	6.0	08.1991	MABT	(Lohse et al., 1993)
	192 ±96			19.2*				02.1992		
Weiss Bank	216			21.6*		0.16	8.0	08.1991		
	120 ±120			16.8*				02.1992		
Tail End	432 ±168			2.4*	fine sand	0.16	5.3	08.1991		
	264 ±120	N.D.	N.D.	0*				02.1992		
Esbjiberg	408 ±216			9.6*		0.06	6.0	08.1991		
	168 ±168			91.2*				02.1992		
Helgoland	0			45.6*	silt	1.28	8.5	08.1991		
	216 ±1220			196.8*				02.1992		
Elbe Rinne	264 ±72			4.8*	muddy sand	0.46	9.2	08.1991		
	288 ±96			31.2*				02.1992		
Frisian Front	624 ±288			16.8*		0.46	9.2	08.1991		
	192 ±72			24.0*				02.1992		
Sylt	81.6 ±64.8			372 ±132*	coarse sand			06.1993	IPT, SIDM	(Jensen et al., 1996)
	11 ±2			44.5 ±13.5*				04.1994		
	3.8 ±1.6	N.D.	N.D.	17 ±4*	fine sand	N.D.	N.D.	04.1994		
	1116 ±924			75 ±39*	muddy sand			03.1993		
	19.5 ±9.5			103.5 ±17.5*				04.1994		
Helgoland	1150 ±700	20 ±5		870 ±100*	fine sand				SIDM	(Marchant et al., 2016)
	210 ±50	250 ±50	N.D.	2280 ±300*	medium sand	N.D.	N.D.	05.2012		
	2980 ±420	110 ±60		520 ±30*	coarse sand					
Sean Gras			24.0	48*	medium sand	0.05	8.1	04.2007	IPT	(Neubacher et al., 2011)
			24.0	72*		0.06	7.4	05.2007		
			0	120*		0.10	8.5	09.2007		
			48.0	144*		0.05	6.6	10.2007		
			0	24*		N.D.	N.D.	04.2008		
Oyster Ground	N.D.	N.D.	24	288*	muddy sand	0.28	10.2	02.2007		
			24	120*		0.22	9.0	04.2007		
			24	120*		0.20	8.4	05.2007		
			120	408*		0.22	9.2	09.2007		
			144	504*		0.23	9.4	10.2007		
			48	144*		0.27	8.7	04.2008		
North Dogger			0	24*	muddy sand	0.45	10.2	02.2007		
			0	96*		0.45	9.4	04.2007		
			24	168*		0.42	9.7	05.2007		
			48	288*		0.46	9.7	09.2007		
			48	264*		0.38	9.6	10.2007		
German Bight / Dogger Bank	N.D.	N.D.	N.D.	20.5 ±4.5**	mud	0.37 ±0.02	N.D.	05.2009	PWMF	(Neumann et al., 2017)
				28.5 ±23.5**		0.16 ±0.12		02.2010		
				8 ±8**	muddy sand	0.13 ±0.10		05.2009		
				12.5 ±12.5**		0.10 ±0.08		02.2010		
				59.5 ±25.5**	sand	0.16 ±0.13		05.2009		
				99 ±35.0**		0.02		02.2010		

566 N.D. – not determined

567 * Denitrification

568 ** NO₃⁻ uptake

Table 2: Characteristics of bottom water and sediment characteristics of the sampled stations in the North Sea (https://doi.org/10.1594/PANGAEA.846041). C_{org} means organic carbon content and TN means total nitrogen content of the surface sediment.

Location	Depth	Sediment core	Incuba-tion time	Sediment type	C_{org}	TN	Porosity	Permea-bility	Temp.	Salinity	OPD
[-]	[m]	[-]	[hours]	[-]	[%]		[-]	[m²]	[°C]	[-]	[mm]
NOAH-A	31.0	1	24	medium sand	0.03 *	≤0.01*	0.37	$1.7 \cdot 10^{-10}$	19.1	33.7	>15
		2	24								
		3	18								
		4	24								
NOAH-C	25.4	1	24	clay/silt	0.73	0.10	0.56	$1 \cdot 10^{-15}$	19.1	32.5	3.6
		2	24								
		3	24								
NOAH-D	38.0	1	18	fine sand	0.21	0.03	0.43	$1.4 \cdot 10^{-13}$	18.9	33.0	2.4
		2	24								
		3	24								
NOAH-E	28.4	1	18	medium sand	0.04	0.01	0.41	$8.8 \cdot 10^{-12}$	18.7	32.4	4.2
		2	18								
		3	24								
		4	24								

* estimated

Table 3: Rates of benthic net NO_3^- and benthic net NH_4^+ fluxes per area, water depth below thermocline (average value of all sediment cores per station) and concentration of dissolved inorganic nitrogen (DIN) in the thermocline. Bottom water concentration of nitrate (cNO_3^-), nitrite (cNO_2^-) and ammonium (cNH_4^+). The concentration of DIN per area was calculated by the multiplication of the water depth below the thermocline with the concentration of DIN. Turnover rates of nitrogen were calculated by the division of DIN per area with the rates of $NH_4^+_{net}$ and $NO_3^-_{net}$ and the effect of sedimentary N release on the reactive nitrogen available for primary production in the water column.

Station	$rNH_4^+_{net} + rNO_3^-_{net}$	Water depth below thermocline	cNO_3^-	cNO_2^-	cNH_4^+	DIN per area	N turnover	sedimentary N support for primary production
[-]	[mmol m^{-2} d^{-1}]	[m]	[μmol L^{-1}]			[mmol m^{-2}]	[days]	[%]
NOAH-A	1.6 ± 0.4	29.5	0.1	< 0.1	0.6 ± 0.2	20.7	10.8 ± 0.3	14.1 ± 4.7
NOAH-C	6.6 ± 1.4	10.0	< 0.1	0.7	2.0 ± 0.2	30.0	3.4 ± 0.1	58.7 ± 10.6
NOAH-D	0.5 ± 0.1	38.0	0.1 ± 0.1	0.1	0.8 ± 0.6	26.6	28.5 ± 0.6	7.1 ± 2.6
NOAH-E	3.2 ± 0.6	10.0	< 0.1	< 0.1	0.3 ± 0.1	3.0	0.9 ± 0.1	26.5 ± 14.3
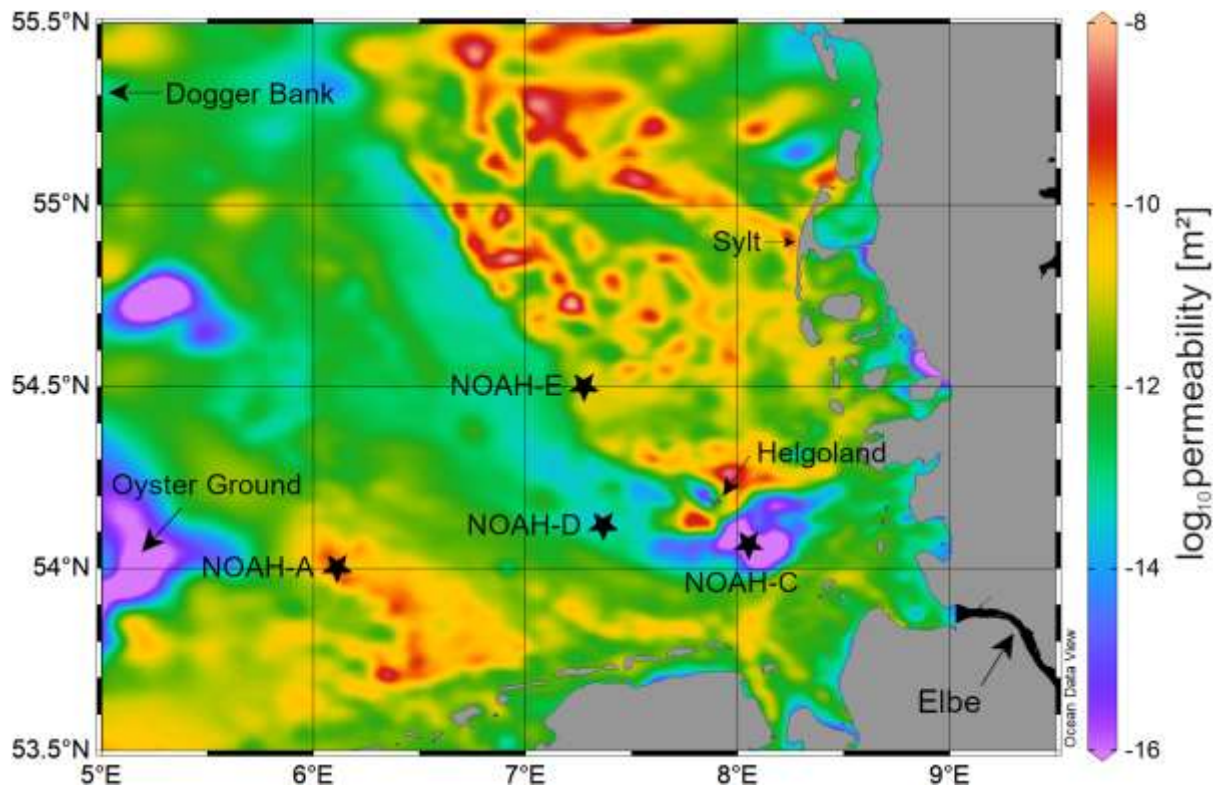
Figure 1: Map showing the sampling stations NOAH-A, NOAH-C, NOAH-D and NOAH-E in the German Bight in the North Sea. Colored areas show the spatial variability of surface sediment permeability (https://doi.org/10.1594/PANGAEA.872712).
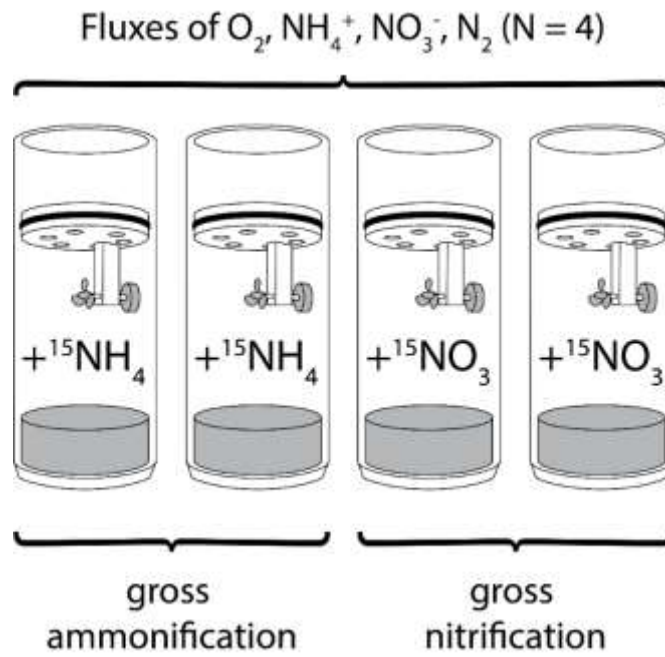
Figure 2: Schematic illustration of the experimental setup. Four sediment cores were incubated to measure benthic fluxes of oxygen, ammonium, nitrate, and N₂. Two of these flux cores were amended with either $^{15}NH_4^+$ or $^{15}NO_3^-$ for the measurement of gross rates of ammonification and nitrification, respectively.
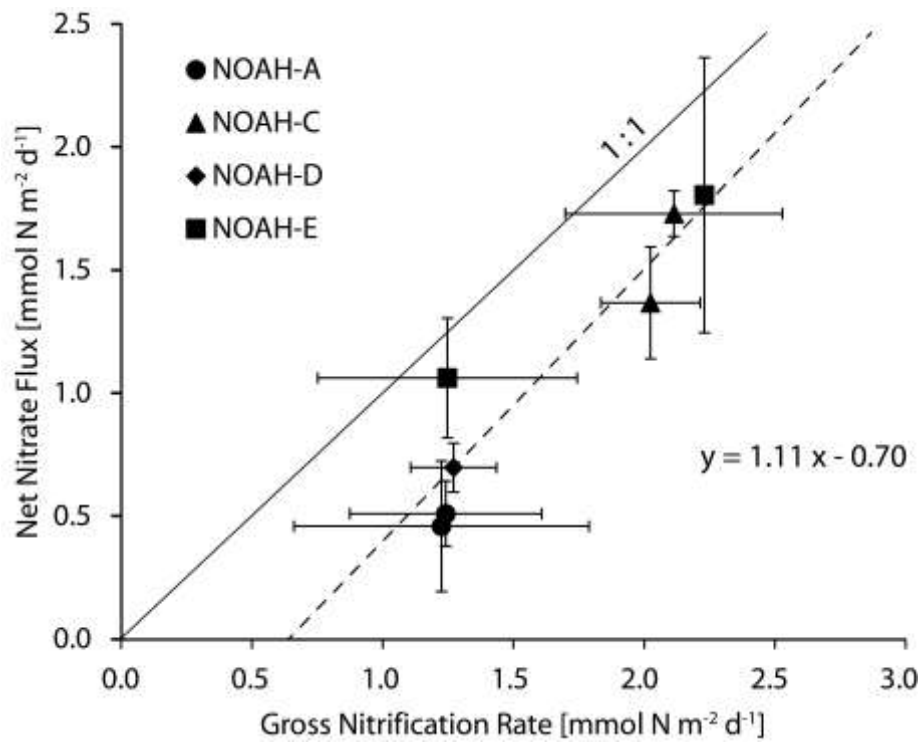
Figure 3: Correlation of gross nitrification rates and actual nitrate fluxes. The solid line indicates the 1:1 ratio, the dashed line indicates the linear regression. The error bars indicate the regression error of individual rates at the 0.95 confidence level.
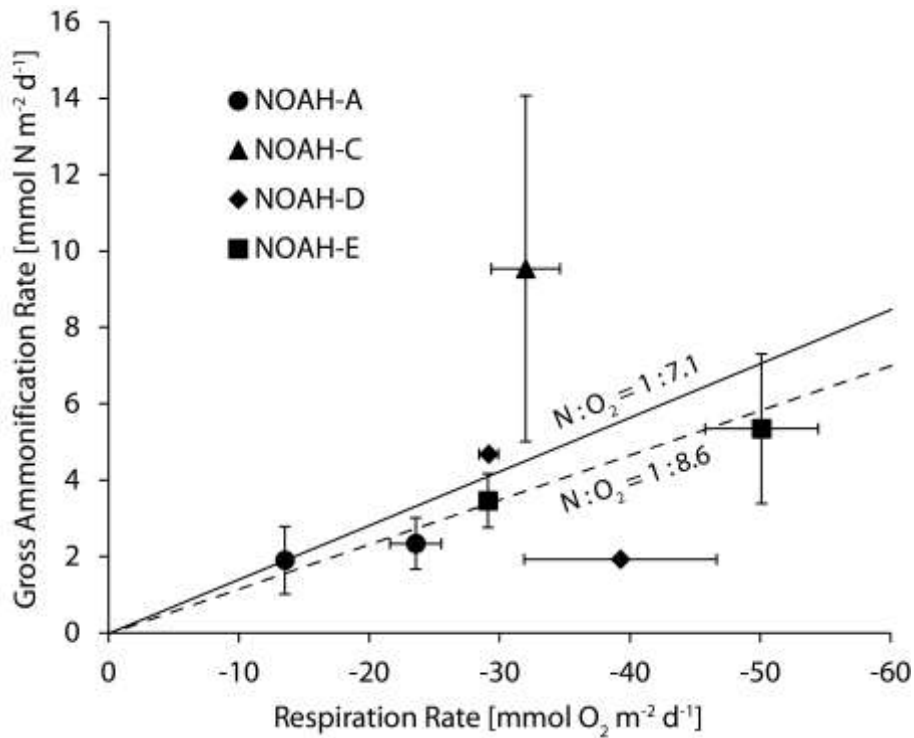
Figure 4: Benthic O₂ fluxes and gross ammonification rates of the sampled stations. The dashed line indicates the Redfield ratio of oxygen and nitrogen (N:O₂ 1:8.625) (Redfield, 1958), and the solid lines indicates the ratio of oxygen and nitrogen determined by the C/N ratio in the North Sea (N:O₂ 1:7.1). The error bars indicate the regression error of individual rates at the 0.95 confidence level.
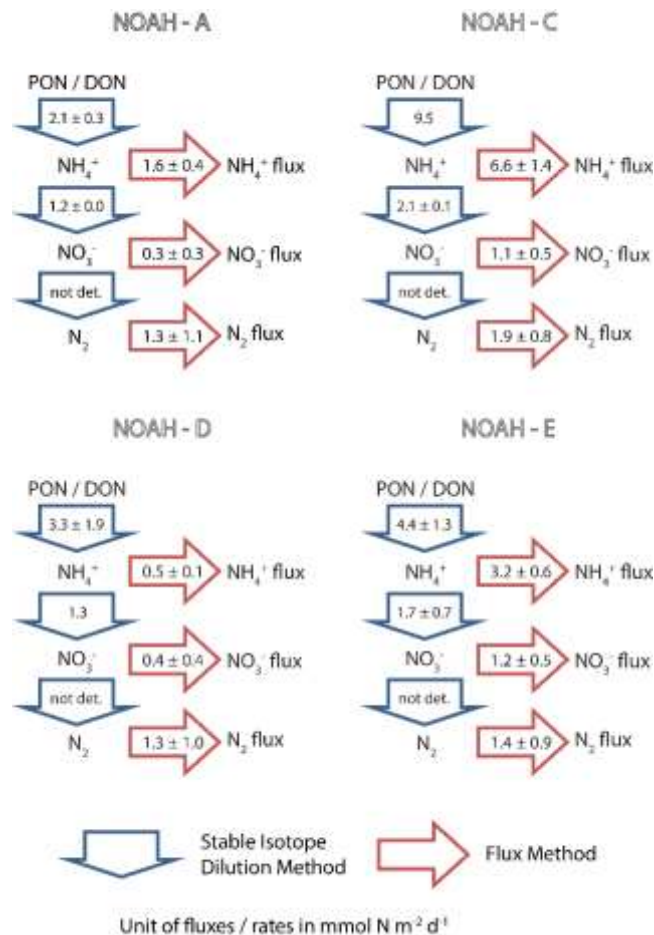
Figure 5: Benthic N-transformation rates (in mmol N m^{-2} d^{-1}) of ammonification (NH_4^+) and nitrification (NO_3^-) as measured by means of stable isotope methods (blue arrows). Simultaneously measured fluxes of ammonium (NH_4^+ flux), nitrate (NO_3^- flux), and N_2 (in mmol N m^{-2} d^{-1}) as measured by the flux method (red arrows).